Nigerian Research Journal of Chemical Sciences, Vol. 6, 2019

THE EFFECTS OF PRECURSOR CONCENTRATIONS AND CALCINATION TEMPERATURES ON HYDROXYAPATITE NANOCRYSTALS SYNTHESIZED AT PHYSIOLOGICAL CONDITION USING WET PRECIPITATION METHOD

*[1]V. Ochigbo, [2]V.O. Ajibola, [2]E.B. Agbaji, [3]A. Giwa, [1]M.O. Ochigbo, [1]J.T. Barminas, [1]B.S. Zuru, [4]P. Mannivasakan, [4]V. Rajendran

[1]National Research Institute for Chemical Technology (NARICT), Zaria-Nigeria

[2]Department of Chemistry, Ahmadu Bello University Zaria-Nigeria

[3]Department of Textile Science and Technology, Ahmadu Bello University Zaria-Nigeria

[4]Centre for Nanoscience and Technology, K.S.Rangasamy College of Technology, Tiruchengode-637 215,

Tamil Nadu, India

*Corresponding Author: ochigbovic@gmail.com

ABSTRACT

In this study, Hydroxyapatite (HA) was synthesized at physiological conditions of pH 7.4 and temperature 37^{o}C using the wet precipitation method. Different concentrations of precursors, viz, 0.5, 1.0, 1.5 and 2.0 M, were studied and calcination was done at 300 ^{o}C, 500 ^{o}C, 800 ^{o}C and 1100 ^{o}C. The results indicated that nano-size HA particles were obtained at all the precursor concentrations. The synthesized hydroxyapatites were characterized by energy dispersive X-ray fluorescence (XRF/EDX), X-ray diffraction (XRD) and Fourier transforms infrared spectroscopic (FT-IR) studies. XRD studies revealed characteristic peaks of hydroxyapatite as confirmed by Joint Committee for Powder Diffraction Standards, International Committee for Diffraction Data (JCPDS) 2001. XRD also revealed the crystalline nature of the powder and the crystallite size (D) and degree of crystallinity (Xc) estimated from pattern using the Derby Scherrer equation indicated that both quantities increases with increase in precursor concentrations and calcination temperatures. FT-IR revealed HA characteristic bands of OH^- and PO_4^{3-}. XRF/EDX revealed the elemental composition of the samples, where the Ca/P ratio was estimated as 1.65; similar to those of natural bone or theoretical value of 1.67 at the precursor concentration of 0.5M and calcination temperature of 300^{o}C.

Keywords: Calcination, hydroxyapatite, nanocrystals, physiological, wet precipitation,

INTRODUCTION

The rapidly growing development of nanotechnology is due to the unique properties of nanocrystalline materials in comparison with their large-grained analogues. Hydroxyapatite (HA)-[$Ca_{10}(PO_4)_6(OH)_2$] is a calcium phosphate ceramic mineral present in the human body. It has for many decades been used as a key material in biomedical engineering as bone implants and prosthesis for dental and bone repair [1]. Biomaterials with nanostructures have unique physicochemical properties and many nano-rooms for the functionalization of biomolecules, and to act as carriers for therapeutics [2]. Morphologically controlled hydroxyapatite nanostructures fulfil multifunctional roles, such as in the form of biosensors [3], photo catalysts [4], carriers for drug delivery [5], appliances in tissue engineering and regenerative medicine [6], as well as membranes for the removal of heavy metals from polluted water [7]. These functional properties of HA strongly depend on their morphology, stoichiometric ratio, crystallinity and crystal size distribution. However, acquiring the desired morphology by controlling the synthesis parameters is difficult and thus it is a challenge to attain the desired morphology with required properties. Hence, researchers have focused on producing HA nanostructures with well distributed and high crystalline nanostructures. Many attempts have being made to improve the powder properties by controlling microstructural morphology. The specific characteristics, crystallization process and bioactivity of diverse nano HA crystals have led to different clinical application [8]. If the crystal can be presented not only as rods and needles but also in spherical and flaky shapes, the nano size HA can be exploited in many other new fields [9]. Nano sized size HA can provide large interfaces, giving high bioactivity and great adsorption capability in the catalysis and separation fields. The important methods for the preparation of HA powders are solid state reaction, precipitation and hydrolysis of calcium phosphates [10]. A processing method was designed to improve and control the powder properties such as crystallinity, particle size, particle size distribution and powder morphology. The processing method was divided into two parts: calcination (to improve the crystallinity), and concentration (to reduce the particle size, narrow the distribution and alter the powder morphology) [11]. In the present work, nano-sized HA powder was synthesized via wet chemical precipitation at physiological conditions of pH and temperature considering the reactant concentrations and calcination temperatures.

MATERIALS AND METHODS

$Ca(NO_3)2{\cdot}4H_2O$, 98%, (MERCK, Germany), NH_4H_2PO4, 99%, (MERCK, Germany), NH_4OH, 25%, (MERCK, Germany) and ultrapure water (Arium 611UF; Sartorius AG) as the starting materials were used as received without any further purification. Firstly, an analytical weighing scale was used to accurately weigh $Ca(NO_3)2{\cdot}4H_2O$ and $NH_4H_2PO_4$ and were respectively dissolved in 500 ml of ultrapure water in a 1000 ml beaker. The pH of each solution was brought up to 7.4 by adding few drops of ammonia solution and the beakers were covered to avoid possible contamination via contact with atmospheric conditions. The temperature of the reaction (37°C) was maintained by a thermostat-controlled water bath. The phosphate solution was added into each of the calcium solution in a drop-wise manner in a beaker to make slurry. The slurry was agitated at 2000 rpm using a digital display thermostat water bath cauldron for 1hr at 37ºC. They were then centrifuged, washed with distilled water until the traces of ammonia were removed. The centrifuged slurry was filtered under mild suction and dried at 80ºC for 24 hours and calcinated in air oven at 300ºC, 500ºC, 800ºC and 1100ºC respectively for 3hrs to produce HA powder. The residue was then made to powders using a mortar and pestle and then characterized via XRF/EDX, FT-IR and XRD.

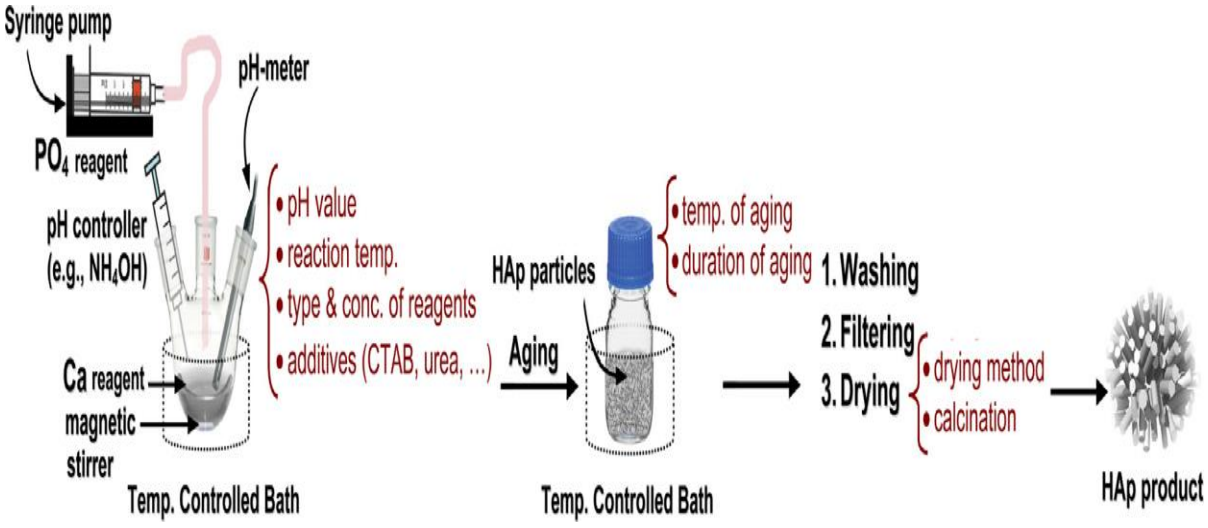

Scheme 3.2: Preparation of HA nanoparticles via conventional chemical precipitation

RESULTS AND DISCUSSION

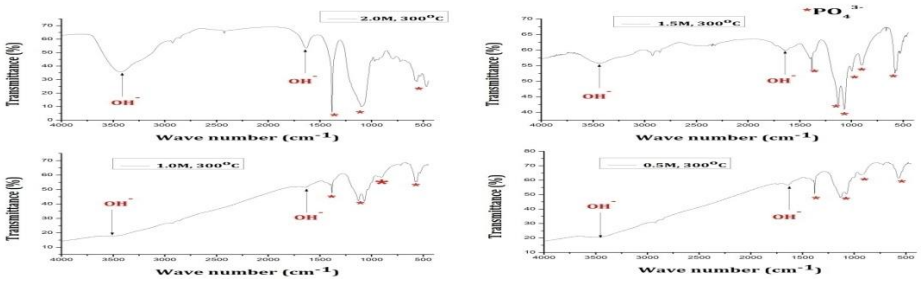

Fig. 1: FTIR spectra of HA synthesized via WT method using different initial precursor concentrations, calcinated at 300°C.

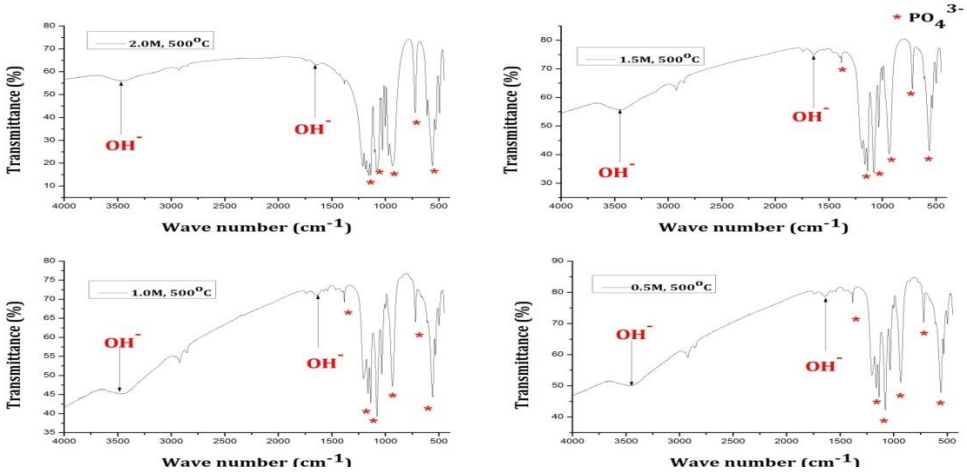

Fig. 2: FTIR spectra of HA synthesized via WT method using different initial precursor concentrations, calcinated at 500°C.

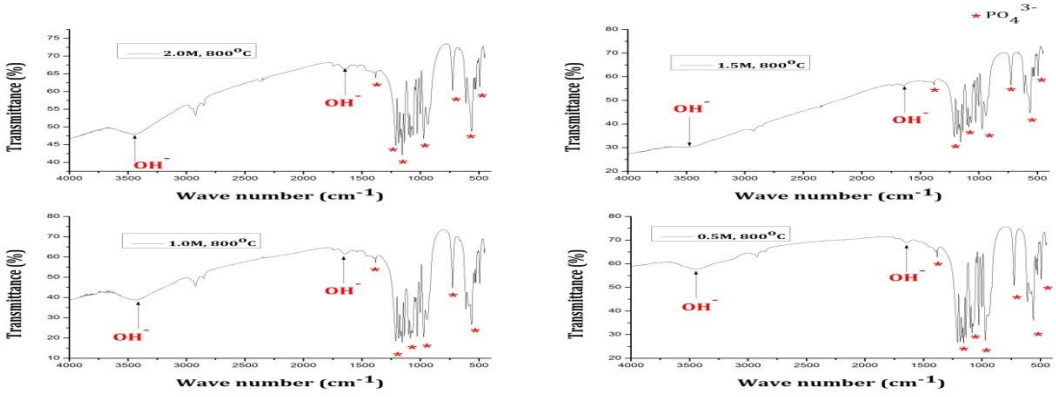

Fig. 3: FTIR spectra of HA synthesized via WT method using different initial precursor concentrations, calcinated at 800°C.

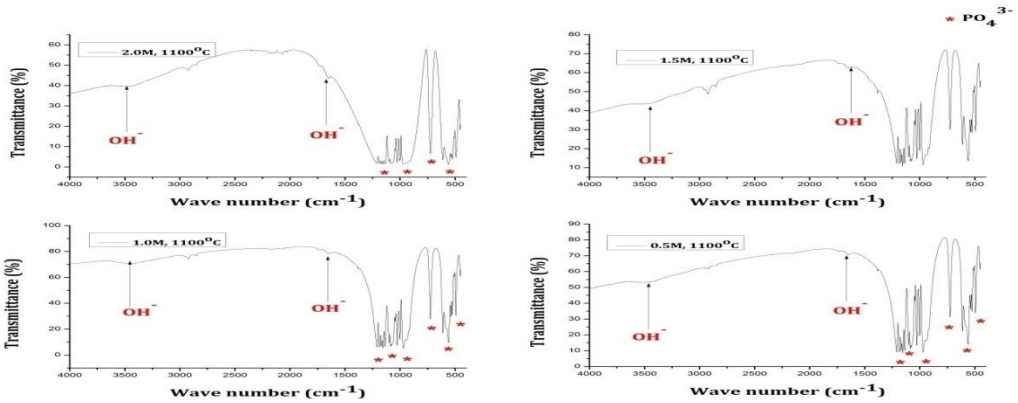

Fig. 4: FTIR spectra of HA synthesized via WT method using different initial precursor concentrations, calcinated at 1100°C.

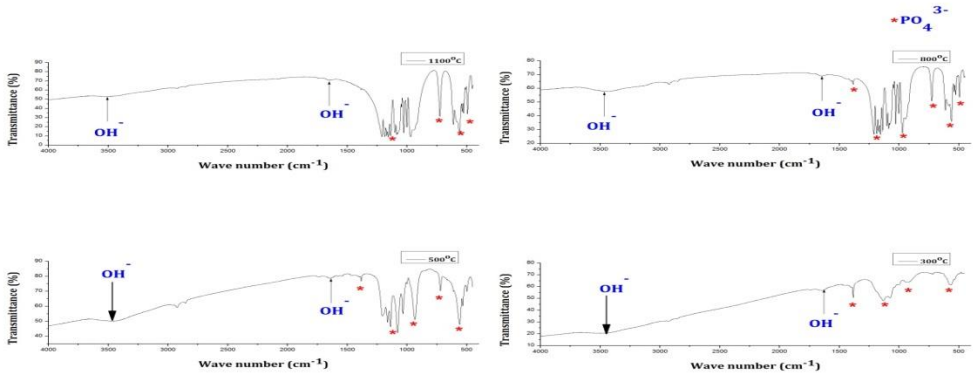

Fig. 5: FTIR spectra of HA synthesized using initial precursor concentration of 0.5M, calcinated at different temperatures.

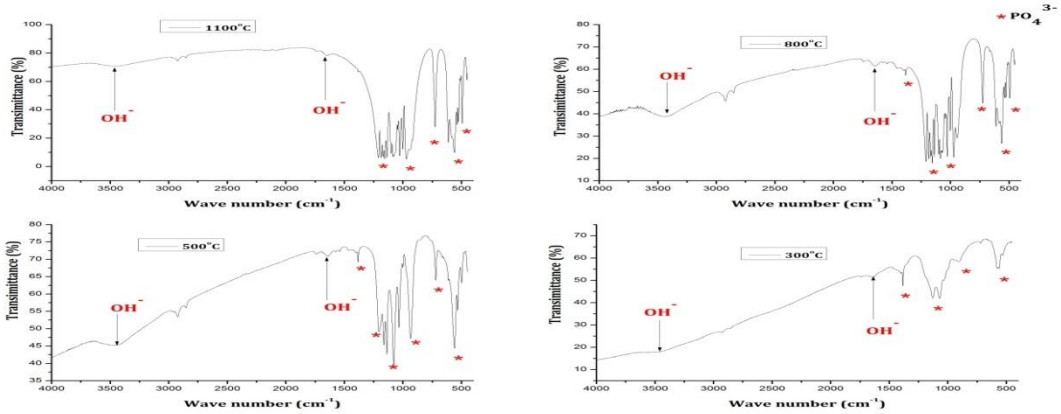

Fig. 6: FTIR spectra of HA synthesized using initial precursor concentration of 1.0M, calcinated at different temperatures.

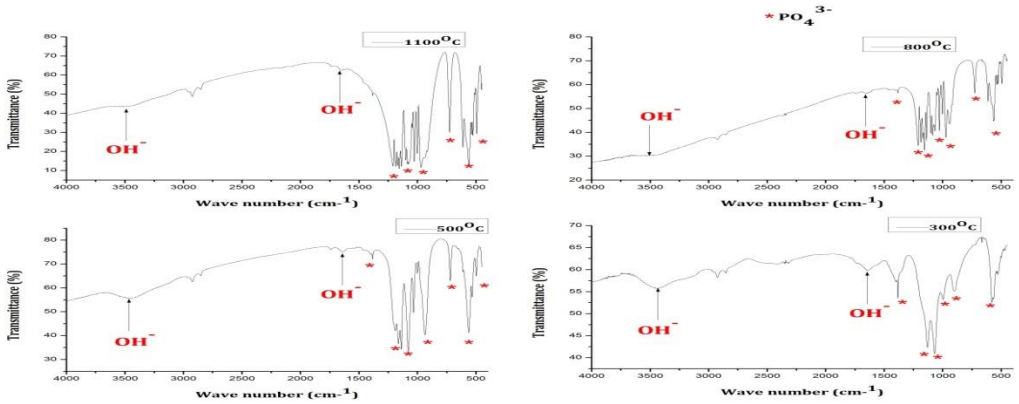

Fig. 7: FTIR spectra of HA synthesized using initial precursor concentration of 1.5M, calcinated at different temperatures.

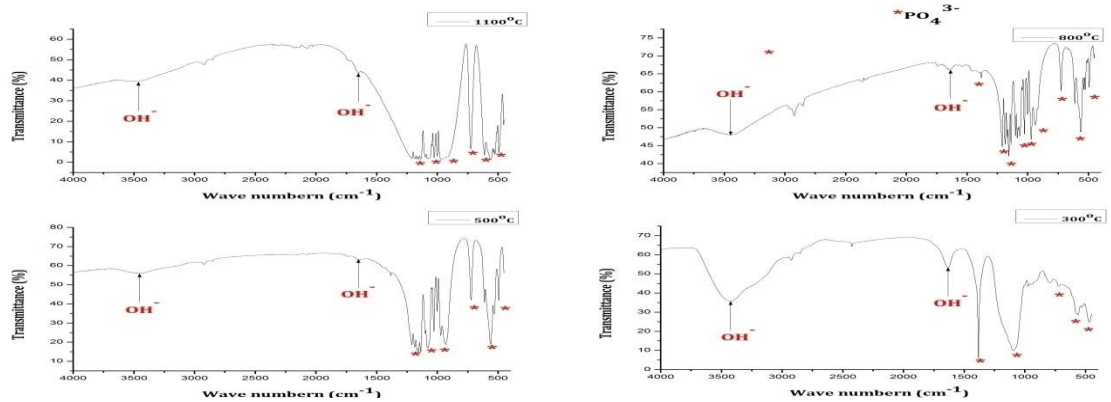

Fig. 8: FTIR spectra of HA synthesized using initial precursor concentration of 2.0M, calcinated at different temperatures.

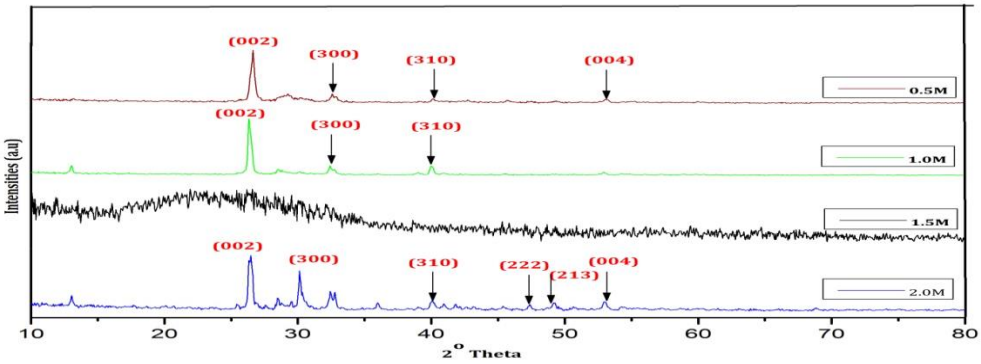

Fig. 9: XRD pattern of HA synthesized via WT method using different initial precursor Concentrations and calcinated at 300°C.

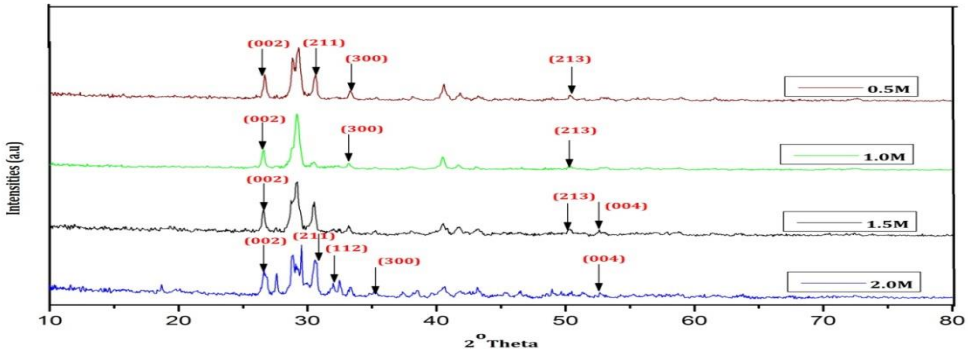

Fig. 10: XRD pattern of HA synthesized via WT method using different initial precursor concentrations and calcinated at 500°C.

Table 1: Major elemental composition and Ca/P ratio of hydroxyapatite synthesized via wet precipitation at various reactant concentrations and calcination temperatures respectively

Reactant concentration (M)	300°C			500°C		
	Ca%	P%	Ca/P	Ca%	P%	Ca/P
0.5	58.863	35.716	1.65	62.239	34.299	1.81
1.0	58.794	36.655	1.60	60.733	34.386	1.77
1.5	60.903	35.393	1.72	66.784	32.577	2.05
2.0	60.303	33.628	1.79	61.708	33.072	1.89

Table 2: The crystallite size and degree of crystallinity of hydroxyapatite synthesized via wet precipitation at various reactant concentrations and calcination temperatures respectively.

Reactant concentration (M)	300°C		500°C	
	Crystallite size D (nm)	Degree of crystallinity (Xc)	Crystallite size D (nm)	Degree of crystallinity (Xc)
0.5	3.7796	0.2268	7.5593	1.8136
1.0	6.0443	0.9286	7.5593	1.8136
1.5	-	-	7.4889	1.8136
2.0	15.1106	14.5089	10.0808	4.2989

The FT–IR spectra of the HA powder (Figures 1 – 8) possess bands for OH^- group in the regions of 3400 – 3500cm^{-1} and 1640cm^{-1}[12, 9] for all precursor concentrations and calcination temperatures, except for calcination temperature of 1100°C. The bands for PO_4^{3-} groups were observed in the region of 1000 – 1500cm^{-1}. The presence of these characteristics' functional groups (OH^- and PO_4^{3-}) in the powder confirmed the formation of hydroxyapatite. These bands became more distinct, narrower with the intensities increased, irrespective of the calcination temperature as the precursor concentration was changed from 0.5M to 2.0M. Decrease in the calcination temperature irrespective of the precursor concentration resulted to an increase in the band intensities, particularly for bands around the 3450 $cm^{-1}$and 1630 cm^{-1} regions corresponding to the OH^- functional groups. This may be attributed to loss of absorbed water as the temperature of calcinations increases. While the bands around 570 cm^{-1}, 1140 cm^{-1}, and 870 cm^{-1}that correspond to the PO_4^{3-} functional group increased with increase in the calcination temperatures, bands around 1420 cm^{-1} corresponding to CO_3^{2-} functional group also decreased with calcinations temperatures from 300 °C to 800°C where it appeared lowest and disappeared at 1100°C calcination temperature. This suggests the decomposition of the carbonate group. However, the increase in band intensities with increase in calcination temperature is attributed to the loss of adsorbed water from the powder, faster particle agglomeration and resultant larger particle size, at high calcination temperatures. Furthermore, the bands in the region of 470-1400 cm^{-1} generally appeared clumsy with non-distinctive bands due to the presence of several phases, particularly for samples calcinated at 800°C and 1100°C for all the precursor concentrations.

The elemental compositions of the synthesized hydroxyapatite particles were ascertained using XRF/EDX (Table 1). The Ca/P ratio increased as calcination temperature increased. This could

be attributed to the fact that at higher temperature of calcination, there was an increase in crystal size as a result of the agglomeration of smaller crystals and its constituent elements [13]. Meanwhile, at a particular calcination temperature, increase in the precursor concentration shows an irregular increase in the Ca/P ratio, an indication of a weak effect of precursor concentration on Ca/P ratio [14]. While comparing the experimental Ca/P ratio to the theoretical (Ca/P=1.67), the hydroxyapatite synthesized using precursor concentrations of 0.5 and 1.5M and calcinated at 300°C gave Ca/P ratio that are in conformity with the theoretical value, suggesting their similarity to the natural apatite than HA prepared at other precursor concentrations and calcination temperatures. This may be attributed to the fact that, at higher temperature of calcination irrespective of the precursor concentrations, hydroxyl group of the hydroxyapatite tend to be lost and thus forms other calcium phosphate minerals like alpha and beta tricalcium phosphate (α and β -TCP) with higher Ca/P ratios. Furthermore, the Ca/P ratio close to 1.67 as seen from 0.5M at 300°C suggests that no CaO content was present and the HA with Ca/P close to 1.75 and above suggests formation of small amounts of CaO [15].

The XRD pattern of the synthesized hydroxyapatite (Figures 9 – 10), indicated that the diffraction patterns gave sharp and clear reflections with varying intensities which confirms the phase purity and crystallinity associated with each sample. The major diffraction peaks located at 2θ = 25.9° (002), 2θ = 53.1° (004), and 2θ = 25.9° (002), 2θ = 53.1° (004) for HA from the hydrothermal and wet precipitation methods were found to match with the International Centre for Powder Diffraction Studies- Joint committee for Powder Diffraction Studies [16] files for calcium phosphate. The predominant HA phase were confirmed as they matched with JCPDS files numbers 00 – 009 – 0432. These data confirmed the major phase as hydroxyapatite particles. The crystallite size and degree of crystallinity (Table 4.3) vary with precursor concentration and the calcination temperatures. The degree of crystallinity increased with temperature of calcination, which was attributed to the increased crystallite sizes implying more crystal planes at high temperature due to particle agglomeration, while at a particular calcination temperature (300^{o}C or 500^{o}C), crystallite size and degree of crystallinity increased with increase in precursor concentration. These variations observed are in agreement with the work reported by [17, 15 and 18]. Furthermore, it was observed that HA calcined at higher temperature (500°C) exhibited high crystallinity. This high crystallinity could be attributed to the fact that high

calcination temperature would lead to an increase in crystal size translating to more crystal planes, as nanocrystals tend to agglomerate forming large crystals, hence, the high crystallinity observed than calcination at lower temperature [19]. However, this high crystallinity has little or lacks bioresorptive potentials, which is the major property of HA as an implant material [20].

In this optimization, the hydroxyapatite prepared using precursor concentration of 0.5M and calcination temperature of 300^{o}C with (Ca/P = 1.65) gave better similarity to those of the natural bone apatite (Ca/P = 1.67), the desired crystallinity and smaller particle size. So, on the basis of Ca\P ratio being closely similar to those of natural bone (Ca\P ═ 1.67) [21], the smaller particle size with reduced crystallinity depicting bioresorptive potentials [3, 22] and the absence of impurities like CaO, α–TCP and β–TCP as observed from the different characterization techniques (FTIR, XRF\EDX and XRD) using the wet chemical methods at physiological conditions for synthesis of HA indicated high purity of the method compared to the use of other synthetic methods like the dry methods and the high temperature processes [15]. 0.5M precursor concentration and calcinations temperature of 300°C were adopted as the optimum conditions for synthesis of biomimetic HA at physiological conditions for the subsequent synthesis.

CONCLUSION

Hydroxyapatite was successfully synthesized at all the precursor concentrations of 0.5, 1.0, 1.5 and 2.0M, by wet precipitation at physiological conditions. As calcinations temperature increased, crystallinity increased and crystal size tends to micron from nano as a result of loss of hydroxyl group.

REFERENCES

1. Cuneyt Tas, A., Korkusuz, F., Timucin, M. & Akkas, N. (1997). An investigation of the chemical synthesis and high-temperature sintering behaviour of calcium hydroxyapatite (HAp) and tricalciumphosphate (TCP) bioceramics. *J. Mater. Sci: Mater. Med*. 8, 91-96.
2. Subbiah, R., Veerapandian, M. & Yun, K.S (2010). Nanoparticles: Functionalization and multifunc-tional applications in biomedical sciences. *Curr. Med. Chem*. 17, 4559-4577.
3. Wang, S., Lei, Y., Zhang, Y., Tang, J., Shen, G. & Yu, R. (2010). Hydroxyapatite nanoarray based cyanide biosensor. *Anal. Biochem*. 398, 191-197.

4. Vukomanovic, M., Zunic, V., Otonicar, M., Repnik, U., Turk, B., Skapin, S. & Suvorov, D. (2012). Hydroxyapatite/platinum bio-photocatalyst: a biomaterial approach to self-cleaning. *J. Mater. Chem.* 22, 10571-10580.

5. Cheng, W.P, Gray, A.I, Tetley, L., Hang, T.L.B, Schätzlein, A.G. & Uchegbu, I.F. (2006). Polyelectrolyte nanoparticles with high drug loading enhance the oral uptake of hydrophobic compounds. *Bio-macromolecules,* 7, 1509-1520.

6. Ebaretonbofa, E. & Evans, J.R.G (2002). High porosity hydroxyapatite foam scaffolds for bone substitute. *J. Porous Mater*. 9, 257-263.

7. Takagi, O, Kuramoto, N., Ozawa, M. & Suzuki, S. (2004). Adsorption/desorption of acidic and basic proteins on needle-like hydroxyapatite filter prepared by slip casting. *Ceramics International*, 30, 139-143.

8. Hench, L.L. (1991). Bioceramics: from concept to clinic, *J Am Ceram Soc*.; 74,1487– 510.

9. Wang, Y. J. Chen,J.D. Wei, K. Zhang, S.H. Wang,X.D. (2006). Surfactant-assisted synthesis of hydroxyapatite particles, *Materials Letters* 60, 3227–3231

10. Thangamani, N., Chinnakali, K. & Gnanam, F. D. (2002). The effect of powder processing on densification, microstructure and mechanical properties of hydroxyapatite, *Ceramics International*, 28: 355-362.

11. KotHApalli, C., Wei, M., Vasiliev, A.M. &.Shaw, T. (2004). Influence of temperature and concentration on the sintering behavior and mechanical properties of hydroxyapatite, *Acta Materialia*, 52: 5655-5663.

12. Liu, J. B., Ye, X. Y. & Wang, H. (2003). The Influence of pH and temperatures on the morphology of hydroxyapatite synthesized by hydrothermal method. *Ceramics International*, 29, 629 – 633.

13. Evis, Z., & Webster, T. J., (2011). Nanosize hydroxyapatite: doping with various ions. *Adv. Appl. Ceram.* 110, 311-320.

14. Raynaud, S., Champion, E., Bernache-Assollant, D. & Thomas, P. (2002). Calcium phosphate apatite with variable Ca/P atomic ratio I. Synthesis, Characterisation and thermal stability of powders. *Biomaterials*, 23: 1065–1072

15. Sanosh, K. P., Chu, M. C., Balakrishnan, A., Kim, T. N. & Cho, S. J. (2009). Utilization of biowaste eggshells to synthesize nanocrystalline hydroxyapatite powders. *Materials*

letters, 63, 2100-2102

16. JCPDS 9-342, ―Hydroxyapatite, Joint Committee for Powder Diffraction Standards, International Committee for Diffraction Data.
17. Syed S. A. A. & Murtaza, Q. (2014). Synthesis and Characterization of nano-hydroxyapatite Powder using Wet chemical Precipitation Reaction. *Journal of material Science & Technology;*30(4): 307–310
18. Bouyer, E., Gitzhofer, F., & Boulos, M. I., (2000). Morphological study of hydroxyapatite nanocrystal suspension. *J. Mater. Sci. Mater. Med.*; 11: 523-531
19. Mobasherpour, I., Heshajin, M. S, Kazemzadeh, A. & Zakeri, M. (2007). Synthesis of naocrystaline hydroxyapatite by using precipitation method. *Journal of Alloys Compounds*, 430-330
20. Gergely, G., Weber, F., Lukacs, I., Illes, L., Toth, A. L., Horvath, Z. E., (2010) Nanohydroxyapatite preparation from biogenic raw materials. *Central Eur J Chem.* 8, 375-81
21. Fatehi, K., Moztarzadeh, F., Soalti-Hashjin, M., Tahriri, M., Rezvannia, M., & Ravarian, R. (2008) *In vitro* biomimetic deposition of apatite on alkaline and heat treated Ti6A14V alloy surface. *Bull Mat Sci*; 31: 101-8.
22. Dorozhkin, S.V. (2010) Nanosized and nanocrystalline calcium orthophosphates. *Acta Biomater*; 6:715–34.